2024 European Control Conference (ECC)
June 25-28, 2024. Stockholm, Sweden

Winch Sizing for Ground-Generation Airborne Wind Energy Systems

Jesse I.S. Hummel[1,*], Tijmen S.C. Pollack[1], Dylan Eijkelhof[1], Erik-Jan van Kampen[1] and Roland Schmehl[1]

***Abstract*— MegAWES is a reference design and simulation framework for ground-generation, fixed-wing airborne wind energy systems with a nominal power output of $3\,\mathrm{MW}$. The winch size of MegAWES is based on a smaller system and needs to be scaled up because the current size leads to unrealistically fast dynamics, which require saturation. However, there is no available method to select an appropriate size for the winch. Additionally, while it has been hypothesized that the size of the winch has a significant effect on the dynamics of the overall system for ground-generation concepts, this effect has not been quantified. In this work, we first analyze the effects of the winch size on the system dynamics using a linearized model. Second, we present a method to find the upper bound for the size of the winch based on a selected maximum tether force overshoot during nominal operation. Third, we apply this method to find an upper bound for the winch size for the MegAWES reference design. Using the nonlinear MegAWES simulation framework, we validated this upper bound. At the upper bound, the system accurately tracked the reference tether force without overshoot and when exceeding our upper bound, the tether force response was oscillatory and overshot its ideal value.**

I. Introduction

Wind is a great resource of renewable energy. The most common method of capturing this energy is with horizontal-axis wind turbines. The wind turbine design is continually improving to increase performance, mostly through taller towers and longer blades [1]. Higher towers generally reach stronger and more constant winds [2] and longer blades can sweep a larger area. This has increased the capacity and capacity factor while lowering costs [1].

Airborne wind energy is a radical new approach to harvesting wind energy that involves the use of tethered flying devices. Loyd [3] first envisioned this concept and calculated that multi-megawatts of power could be extracted from higher altitude winds using this method. The flying devices are attached to a ground station with a tether and fly mostly perpendicular to the wind in circles or figures of eight. There are four popular system concepts, as shown in Fig. 1 [4]. In this work, ground-generation (ground-gen) fixed wing systems are considered. Fixed wing refers to the rigid materials used for the construction of the kite. Ground-gen operation uses a ground-based generator and performs pumping cycles with the kite that comprise two phases: the traction phase (energy-generating) and the retraction phase (energy-consuming). During the traction phase, the pull exerted by the kite on the tether is converted into electricity by rotating the ground-based winch and generator. Once the maximum length of the tether is reached, the kite is retracted. Since the kite can be placed in an aerodynamically favorable position during the retraction phase, it consumes only a fraction of the energy produced in the traction phase [5].

The systems currently in development range from tens to hundreds of kilowatts. However, to get to utility-scale power production, individual systems will need to be scaled up to several MW's per unit [6]. "MegAWES" is the first publicly available, multi-megawatt, ground-gen, fixed-wing reference model and simulation framework [7], [8]. It is intended for cross-validation and benchmarking. It has a wing surface area of $150\,\mathrm{m}^2$ and a nominal power output of $3\,\mathrm{MW}$. The winch design (defined by its radius and inertia) is based on a smaller system and has not been scaled up yet, which leads to tracking errors in the tether force and unrealistically fast winch dynamics which often need saturation [7]. However, there is no existing method to select an appropriate size of the winch to ensure accurate tracking of the tether force. Furthermore, while it has been hypothesized that the size of the winch has a significant effect on the system dynamics [9], we are not aware of any publications that systematically investigate these effects.

This paper aims to address these challenges with the following three contributions:

1) An analysis of the effects of the size of the winch on the dynamics of the system,
2) A method to determine the upper bound on the winch size,
3) A proposed upper bound on the winch size for the MegAWES reference design.

The paper is structured as follows: In Section II, we derive the linear system dynamics, analyze the effect of the winch size, present a method to determine the upper bound for the winch size, and explain the setup in the nonlinear MegAWES simulation framework. The presented winch sizing method is applied to the MegAWES reference design in Section III, where it is also validated using the nonlinear MegAWES simulation framework. Section IV concludes this work.

II. Methods

This section starts with an analytical derivation of the winch dynamics. The equations are then linearized to analyze the effect of the winch size on the system dynamics. This analysis leads to a method for selecting an appropriate winch size. Lastly, the simulation setup in the nonlinear MegAWES simulation framework is explained which is used for validation.

[1]Faculty of Aerospace Engineering, Delft University of Technology, 2629 HS Delft, The Netherlands.
*Corresponding author, email: j.i.s.Hummel@tudelft.nl

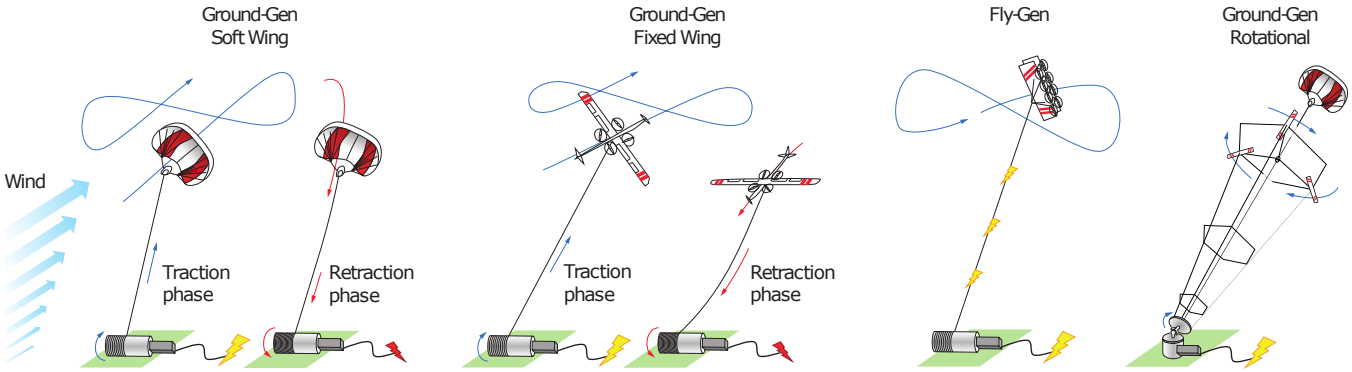

Fig. 1. Visualization of the four most advanced airborne wind energy system concepts. From left to right: soft wing with ground-gen, fixed wing with ground-gen, fixed wing with fly-gen, and the rotating kite concept. Figure obtained from [4].

The source code used for this section is available at [10].

A. Derivation of the Winch Dynamics

In this work, the winch refers to the drum on which the tether spools, the drivetrain, and the generator. This is modeled as a single rotating body with a given inertia J and radius r, similar to [8] but without viscous friction. This is done to simplify the equations later and is allowed because the friction torque is much smaller than the tether force and control torque. It is furthermore assumed that the radius is constant despite the spooling of the tether. The spooling adds small and slow changes in the radius so these dynamics are negligible.

With these assumptions, two moments act on the winch: the tether force multiplied by the radius of the winch and the winch control torque, both of which are explained next. The block diagram for this system is shown in Figure 2.

We use the quasi-steady model from [11] to calculate the tether force. We assume that the wind speed is parallel to the tether, thus neglecting cosine losses, and neglect the mass of the kite. All these variables would affect the kite's apparent wind speed, in particular the course angle, since gravity speeds the kite up when flying downwards and slows it down when going upwards. Instead of modeling these effects individually, we use the input "equivalent" wind speed of the quasi-steady model as a proxy for all these effects. The tether force is then given by [11]

$$\begin{aligned} &F_\mathrm{t} = \mathscr{C}(v_\mathrm{w} - v_\mathrm{r})^2, \\ &\text{where} \\ &\mathscr{C} = \frac{1}{2}\rho S C_\mathrm{L} E_\mathrm{eq}^2 \left(1 + \frac{1}{E_\mathrm{eq}}\right)^{\frac{3}{2}}, \end{aligned} \tag{1}$$

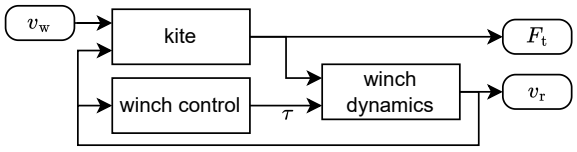

Fig. 2. Block diagram describing the model with wind speed as input and tether force and reel-out speed as outputs.

where F_t denotes the tether force, v_w the equivalent wind speed, v_r the reel-out speed, ρ the air density, S the reference wing area, C_L the lift coefficient, E_eq the equivalent lift-to-drag ratio (taking the tether drag into account). The constant $\mathscr{C}$ is related to the performance and size of the kite.

The winch control torque is chosen with a feedback strategy that aims to keep the system at its optimal reel-out factor f^*, where $f = {}^{v_\mathrm{r}}/_{v_\mathrm{w}}$. An optimal reel-out factor of ⅓ [3] is assumed. This is not optimal when considering the reel-out and reel-in phase together [12]. However, this is outside the scope of this work and would not change our conclusions. The control law can then be formulated by assuming steady-state reeling where the winch control torque and the torque arising from the tether force are in equilibrium when the optimal reel-out factor is reached, see [11] for the derivation. This results in a winch control curve where the optimal tether force can be calculated as a function of reel-out speed, see Fig. 3. This curve is sometimes called the "optimal force-squared speed manifold" [13]. The control torque is then simply the optimal tether force multiplied by the radius:

$$\tau = 4\mathscr{C} v_\mathrm{r}^2 r, \tag{2}$$

where τ denotes the winch control torque.

From these pieces, the closed-loop state equation for the system is derived

$$\begin{aligned} J\dot{\omega} &= \sum M \\ J\frac{\dot{v}_\mathrm{r}}{r} &= \mathscr{C}(v_\mathrm{w} - v_\mathrm{r})^2 r - 4\mathscr{C} v_\mathrm{r}^2 r \\ \dot{v}_\mathrm{r} &= \frac{\mathscr{C}}{K_\mathrm{w}}(v_\mathrm{w}^2 - 2v_\mathrm{w}v_\mathrm{r} - 3v_\mathrm{r}^2), \\ &\text{where} \\ K_\mathrm{w} &= \frac{J}{r^2}, \end{aligned} \tag{3}$$

where ω denotes the rotation speed of the winch. Furthermore, the winch sizing parameter K_w is introduced, which can be physically interpreted as being equal to the mass of a thin-walled cylinder with radius r and inertia J. Since friction was neglected, all parameters related to the size of the winch can be collected in this single parameter, that only appears once in the equations of motion.

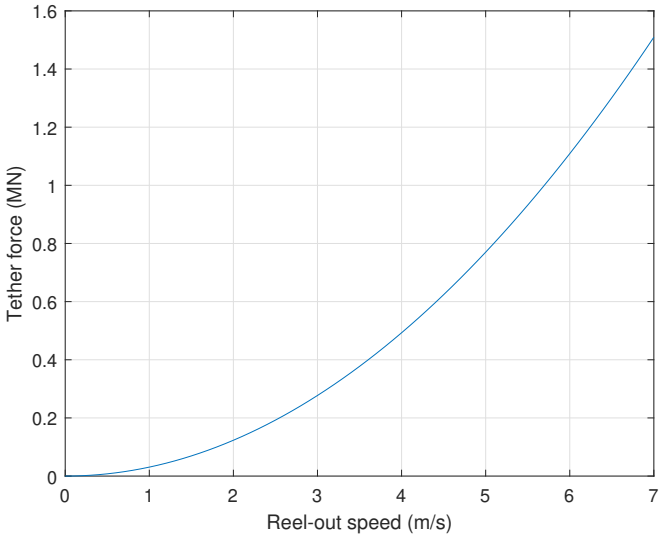

Fig. 3. Winch control curve, showing the optimal (quasi-steady) tether force as a function of reel-out speed for a reel-out factor of 1/3.

B. Linearization of the the winch model

The nonlinear state equation (3) is linearized around a trim point where the tether force and control torque are in equilibrium and thus $\dot{v}_\mathrm{r} = 0$. The optimal torque controller is designed such that this equilibrium occurs at the optimal reel-out factor. Thus at the trim condition

$$v_{\mathrm{r}0} = f^* v_{\mathrm{w}0} = \frac{1}{3} v_{\mathrm{w}0} \tag{4}$$

holds.

The linear state equation then simplifies to

$$\dot{v}_\mathrm{r} \approx \frac{\mathscr{C}}{K_\mathrm{w}} \left(\frac{4}{3} v_{\mathrm{w}0} \Delta v_\mathrm{w} - 4 v_{\mathrm{w}0} \Delta v_\mathrm{r}\right). \tag{5}$$

Next, we take the Laplace transform to get the transfer function from equivalent wind speed to reel-out speed:

$$\frac{V_\mathrm{r}(s)}{V_\mathrm{w}(s)} = \frac{4\mathscr{C} v_{\mathrm{w}0}}{3K_\mathrm{w} s + 12\mathscr{C} v_{\mathrm{w}0}}. \tag{6}$$

This procedure is repeated for the output equation (1) for the tether force, resulting in

$$\frac{F_\mathrm{t}(s)}{V_\mathrm{w}(s)} = \frac{12\mathscr{C} v_{\mathrm{w}0} K_\mathrm{w} s + 32\mathscr{C}^2 v_{\mathrm{w}0}^2}{9K_\mathrm{w} s + 36\mathscr{C} v_{\mathrm{w}0}}. \tag{7}$$

The nonlinear system described by Fig 2 has now been linearized to two transfer functions describing the reel-out speed (6) and tether force (7) as a function of equivalent wind speed.

C. Effect of the Winch Size on the Dynamics

The pole of this system is located at

$$s = -\frac{4\mathscr{C} v_{\mathrm{w}0}}{K_\mathrm{w}}. \tag{8}$$

As previously implied by [11], this shows that the optimal winch control law described by (2) results in an asymptotically stable system because the parameters $\mathscr{C}$, $v_{\mathrm{w}0}$, and K_w are positive. The transfer function from equivalent wind speed to reel-out speed (6) has a time constant of $K_\mathrm{w}/(4\mathscr{C} v_{\mathrm{w}0})$ and dc-gain of 1/3. As expected, the time constant is high for large winch sizing parameters and low for smaller winch sizing parameters. Furthermore, the time constant is highly dependent on the trim equivalent wind speed, where at higher wind speeds, the system reacts faster. This is because the winch control law (2) is more responsive at high reel-out speeds because the slope on the winch control curve (Fig. 3) is steeper there, thus leading to a larger change in torque for a similar change in reel-out speed.

The transfer function of equivalent wind speed to tether force (7) has a zero at

$$s = \frac{8\mathscr{C} v_{\mathrm{w}0}}{3K_\mathrm{w}} = \frac{2}{3} s_\mathrm{pole}. \tag{9}$$

Since the location of the zero is always closer to the origin than the pole, an increase in tether force overshoot is unavoidable above certain input frequencies. This observation will be used later when we present the winch sizing method.

The transfer functions of the reel-out speed (6) and tether force (7) are normalized by dividing them by the steady-state magnitude to a step response, which is computed using the final value theorem. The steady-state magnitude for the tether force to a step input on the equivalent wind speed is equal to

$$F_{t,\mathrm{final}} = \lim_{s\to 0} s \frac{F_\mathrm{t}(s)}{V_\mathrm{w}(s)} \frac{1}{s} = \frac{32\mathscr{C} v_{\mathrm{w}0}}{36}. \tag{10}$$

This procedure is repeated for the state equation (6).

The Bode plot of these normalized transfer functions is shown in Fig. 4. The numerical values used are summarized in Table I. The values related to the MegAWES reference design are obtained from [7].

From Fig. 4 it is observed that the tether force magnitude increases at high input frequencies, with up to 50 % overshoot (note that the y-axis uses absolute units instead of decibels). This occurs because the winch cannot adapt its reel-out speed sufficiently quickly, as indicated by its magnitude going towards zero and its phase going towards $-90°$. This tether force overshoot would increase the probability of tether rupture or lead to more conservative operation and should thus be avoided.

A second observation is that the reel-out speed and tether force phases start to diverge above a certain input frequency.

TABLE I
PARAMETERS USED FOR ANALYSIS.

MegAWES parameters [7]	
S	$150.45\,\mathrm{m}^2$
C_L	1.8
E_eq	6.7
J	$32\,\mathrm{kg\,m}^2$
r	$0.4\,\mathrm{m}^2$
environment	
ρ	$1.225\,\mathrm{kg/m}^3$
trim condition	
$v_{\mathrm{w}0}$	$10\,\mathrm{m/s}$

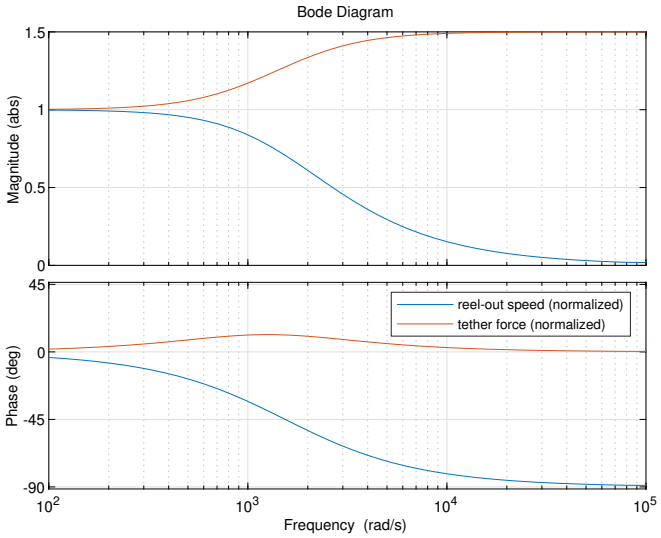

Fig. 4. Bode plot of the normalized tether force and power output. As the equivalent wind speed input frequency goes up, the reel-out speed starts to lag and has a lower magnitude causing the tether force oscillation to increase in magnitude, leading to tether force overshoot.

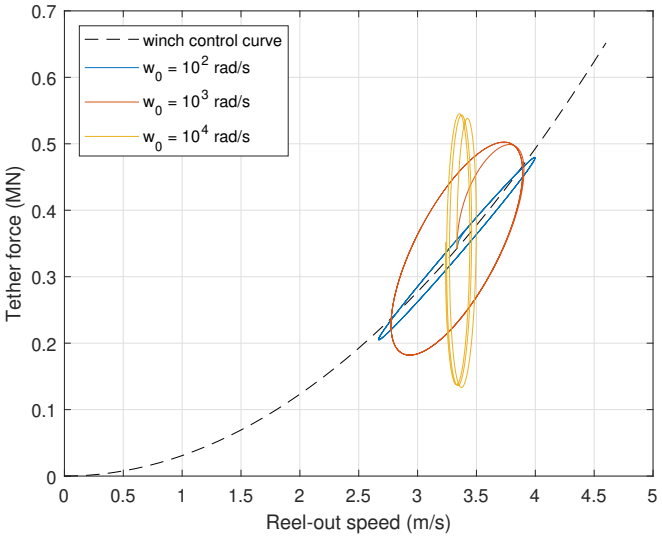

Fig. 5. Response of the linearized system on the winch control curve for different input frequencies. When the equivalent wind speed changes slowly, the winch can follow the optimal winch control curve. The tracking deteriorates as the input frequency goes up.

This causes the system to diverge from the optimal winch control curve (previously shown in Fig. 3). This effect is visualized by showing the time response of the linearized system on the winch control curve for three different input frequencies in Fig 5 by plotting the time response of the reel-out speed on the x-axis and the time response of the tether force on the y-axis. At low input frequencies, the system closely follows the prescribed winch control curve. However, as the input frequency increases, the response oscillates around it, thus no longer correctly tracking the prescribed curve. This situation should thus be avoided.

So, the system should have a sufficiently small time constant to handle the fastest expected change in equivalent wind speed. Then, the system would not experience a tether force overshoot or poor tracking of the winch control curve.

In these examples, the excitation frequencies are rather high. This is because the bandwidth of the MegAWES winch is $1.54\times10^3\,\mathrm{rad/s}$ at a trim equivalent wind speed of $10\,\mathrm{m/s}$. As discussed by [14], the winch size had not been scaled up from the smaller reference system on which the MegAWES reference design is based, which led to tracking errors in the tether force and unrealistically fast winch dynamics that often needed saturation. So, the winch should be scaled up to decrease its bandwidth. Thus, the winch sizing method proposed in the next section aims to find an upper bound on the size, achieving the lowest bandwidth that still satisfies certain operational requirements.

D. Winch Sizing Method

To find suitable values for the winch sizing parameter, a limit on the magnitude of the transfer function of the normalized tether force is set at the highest expected frequency of the equivalent wind speed. For airborne wind energy systems, this frequency is related to the period of a circle or halve the period of a figure-of-eight because at this frequency the system will experience a change in apparent wind speed (due to gravity). We denote this frequency by w_0. The magnitude of the transfer function for the normalized tether force at this frequency is

$$\left\| \frac{F_{\mathrm{t,normalized}}(jw_0)}{V_{\mathrm{w}}(jw_0)} \right\| = \sqrt{\frac{9K_{\mathrm{w}}^2 w_0^2 + 64\mathscr{C}^2 v_{\mathrm{w0}}^2}{4K_{\mathrm{w}}^2 w_0^2 + 64\mathscr{C}^2 v_{\mathrm{w0}}^2}}. \tag{11}$$

This equation can be rewritten to arrive at the following closed-form solution for the winch sizing parameter:

$$K_{\mathrm{w}} = \frac{8\mathscr{C} v_{\mathrm{w0}}}{\omega_0}\sqrt{\frac{f_{F\mathrm{t}}^2 - 1}{9 - 4f_{F\mathrm{t}}^2}} \quad \text{where} \quad f_{F\mathrm{t}} = \left\| \frac{F_{t,\mathrm{normalized}}(jw_0)}{V_{\mathrm{w}}(jw_0)} \right\|, \tag{12}$$

and denotes the desired maximum tether overshoot as a fraction of the ideal tether force.

By setting a desired maximum tether force overshoot at the highest expected frequency of the equivalent wind speed, an upper bound on the size of the winch can be found. In the next section, this method will be used to scale up the winch of MegAWES, as recommended by [14]. Furthermore, these analytical results will be verified in the nonlinear MegAWES simulation framework, explained next.

E. Simulation Setup

The MegAWES simulation framework offers both 3DOF (point-mass) and 6DOF dynamics. It is a nonlinear simulation using a lookup table for aerodynamic coefficients, a high-stiffness tether model based on [15], and a winch that is modeled similarly as in this work, but with viscous friction. It uses a control architecture based on [16]. The winch controller keeps the tether force constant when the wind speed does not change. This is different than the control

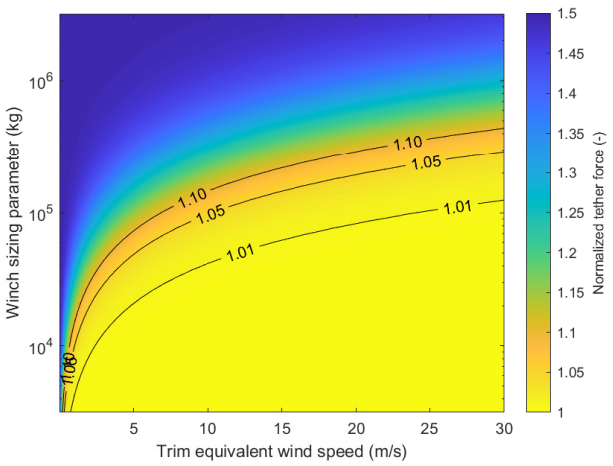

Fig. 6. Normalized tether force as a function of trim equivalent wind speed and winch sizing parameter. The system has a low tether force overshoot at high trim equivalent wind speeds and/or low winch sizing parameters.

law (2) assumed in this work and causes power fluctuations [16] since the equivalent wind speed fluctuates for large-scale systems. So, the control implementation from [17] is used, which uses the same optimal torque control law assumed in this work. Furthermore, they implemented a kite tether force controller that limits peak power, allowing the system to stay on the winch control curve when the tether force limit is reached. This is currently only implemented for the 3DOF dynamics at a wind speed of $22\,\mathrm{m/s}$, so that will be the test condition for this work.

III. Results and Discussion

This section starts with a calculation of the upper bound for the winch sizing parameter for MegAWES. From this, suitable values for the inertia and radius of the winch can be calculated. This new winch size will then be tested in a nonlinear 3DOF simulation of MegAWES and compared to a winch size above the proposed upper bound.

A. Winch Sizing for MegAWES

MegAWES completes a figure-of-eight roughly once every 40 seconds [7]. So the apparent wind speed oscillates with a period of 20 seconds, or at a frequency of $0.05\,\mathrm{Hz}$. To ensure that the system can adapt to slightly faster variations than this fundamental frequency, and account for model uncertainties, the input frequency is multiplied by a factor of 3 and set at $0.15\,\mathrm{Hz}$.

At this frequency, the normalized tether force overshoot is calculated for different trim equivalent wind speeds and winch sizing parameters and is shown in Fig. 6. This visualizes (11) for the MegAWES system. As discussed in Section II, the figure shows that the system achieves low overshoot at high trim equivalent wind speeds and/or small winch sizing parameters.

The upper limit is found at low trim equivalent wind speeds, so the requirement on tether force overshoot is set at $1\,\%$ at a trim equivalent wind speed of $10\,\mathrm{m/s}$ (the cut-in wind speed of MegAWES [7]). Using (12), the upper bound for the winch sizing parameter comes out to $4.2 \times 10^4\,\mathrm{kg}$. This winch sizing parameter can be achieved with an infinite number of combinations of radius and inertia. In this work, we set the radius of the winch to $2.0\,\mathrm{m}$ resulting in an inertia of $1.7 \times 10^5\,\mathrm{kg\,m^2}$.

The radius is identical to a different $5\,\mathrm{MW}$ reference system from [18]. The inertia of the generator of the National Renewable Energy Laboratory (NREL) $5\,\mathrm{MW}$ reference wind turbine is $534\,\mathrm{kg\,m^2}$ about the high-speed shaft [19]. When including the 97:1 gearbox, the apparent inertia of the generator is $51\,809\,\mathrm{kg\,m^2}$. This is below the inertia proposed in this work for MegAWES. So the generator and gearbox combination from the NREL $5\,\mathrm{MW}$ turbine would satisfy the tether force overshoot requirement when used in an airborne wind energy system the size of MegAWES. This suggests that wind turbine components could be used in airborne wind energy systems without exceeding the winch sizing parameter.

B. Validation

The MegAWES simulation framework with the control architecture from [17] is used, as explained in Subsection II-E. The effect of going over the upper bound of the winch size will be shown by analyzing two test cases: One using the proposed upper bound from this work and one with a winch which is three times bigger than the proposed upper bound, as summarized in Table II.

The response during the traction phase of the two cases is plotted on the winch control curve and shown in Fig 7. When using our proposed upper bound, the system follows the ideal curve closely while being over the upper bound makes the system oscillate around the ideal curve, as previously predicted by the linear analysis, see Fig. 5. Selecting the winch size parameter above the upper bound thus leads to an overshoot in the tether force and poor tracking of the desired winch control curve because the winch cannot respond fast enough to changes in the equivalent wind speed.

Even though the presented method to set an upper bound on the size of the winch used several simplifying assumptions, it correctly predicts the upper bound on winch size when the performance starts to deteriorate in a nonlinear 3DOF simulation.

IV. Conclusion

The winch size is an important design parameter for the dynamics of ground-generation airborne wind energy systems. Using a linear model, a closed-form solution was derived to find the upper bound for the winch sizing parameter (defined as J/r^2) by defining a maximum tether

TABLE II
Winch size for the two test cases.

	upper bound	over upper bound
K_w (kg)	4.2×10^4	12.6×10^4
r (m)	2.0	2.0
J ($\mathrm{kg\,m^2}$)	1.7×10^5	5.1×10^5

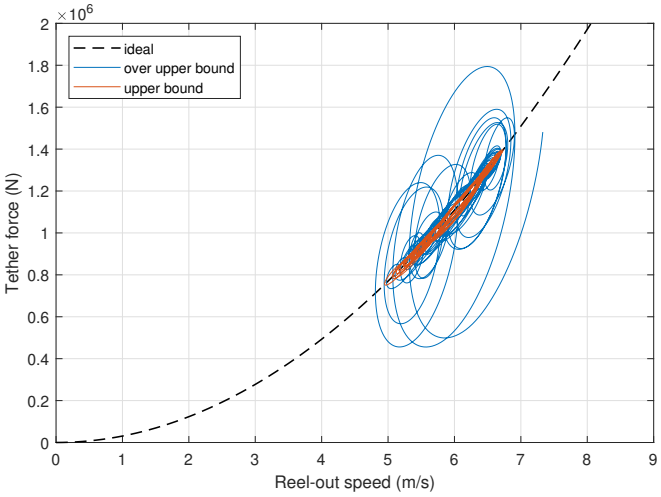

Fig. 7. Response using the 3DOF MegAWES simulation on the winch control curve during the traction phase for the two test cases. At the upper bound, the system follows the optimal winch control curve. The tracking deteriorates when the inertia is increased, as predicted by the linear model.

force overshoot. The upper bound is found when the trim equivalent wind speed is low, and the frequency of the change in apparent wind speed is high, which can arise due to speed variations over the flown trajectory. For MegAWES, the winch sizing parameter has an upper bound of $4.2 \times 10^4\,\mathrm{kg}$ when setting the maximum tether force overshoot to $1.0\,\%$ at a trim wind speed of $10\,\mathrm{m/s}$ (the cut-in wind speed of MegAWES) at an equivalent wind speed frequency of $1.5\,\mathrm{Hz}$ (three times the apparent wind speed frequency experienced by MegAWES in simulation). This winch sizing parameter can be realized with a radius of $2.0\,\mathrm{m}$ and inertia of $1.7 \times 10^5\,\mathrm{kg\,m^2}$. This new winch size was tested using a nonlinear 3DOF simulation. With the selected winch size, the system tracks the winch control curve well. When increasing the winch inertia by a factor of three, the response showed an oscillatory behavior around the winch control curve, as predicted by the linear analysis. In addition, its peak tether force was much higher, validating the presented winch sizing method.

In future work, other inputs besides the main oscillation in apparent wind speed, such as turbulence and operational requirements around the transitions between traction and retraction, should be analyzed. This could further reduce the upper bound on the winch size. Alternatively to this control strategy, the lag of the winch can be compensated for with an additional control loop. However, this controller would come with additional control effort which would increase power fluctuations. Future research could investigate this trade-off.

References

[1] "Annual Report 2020," IEA Wind TCP, Tech. Rep., Aug. 2021.

[2] C. L. Archer and K. Caldeira, "Global Assessment of High-Altitude Wind Power," *Energies*, vol. 2, no. 2, pp. 307–319, May 2009.

[3] M. L. Loyd, "Crosswind kite power (for large-scale wind power production)," *Journal of Energy*, vol. 4, no. 3, pp. 106–111, May 1980.

[4] H. Schmidt, V. Leschinger, F. J. Müller, G. De Vries, R. J. Renes, R. Schmehl, and G. Hübner, "How do residents perceive energy-producing kites? Comparing the community acceptance of an airborne wind energy system and a wind farm in Germany," *Energy Research & Social Science*, vol. 110, p. 103447, Apr. 2024.

[5] C. Vermillion, M. Cobb, L. Fagiano, R. Leuthold, M. Diehl, R. S. Smith, T. A. Wood, S. Rapp, R. Schmehl, D. Olinger, and M. Demetriou, "Electricity in the air: Insights from two decades of advanced control research and experimental flight testing of airborne wind energy systems," *Annual Reviews in Control*, vol. 52, pp. 330–357, 2021.

[6] L. Fagiano, M. Quack, F. Bauer, L. Carnel, and E. Oland, "Autonomous Airborne Wind Energy Systems: Accomplishments and Challenges," *Annual Review of Control, Robotics, and Autonomous Systems*, vol. 5, no. 1, pp. 603–631, May 2022.

[7] D. Eijkelhof and R. Schmehl, "Six-degrees-of-freedom simulation model for future multi-megawatt airborne wind energy systems," *Renewable Energy*, vol. 196, pp. 137–150, Aug. 2022.

[8] D. Eijkelhof, U. Fasel, and S. Rapp, "MegAWES (3DoF & 6DoF kite dynamics)," https://github.com/awegroup/MegAWES, 2021.

[9] M. Erhard and H. Strauch, "Flight control of tethered kites in autonomous pumping cycles for airborne wind energy," *Control Engineering Practice*, vol. 40, pp. 13–26, July 2015.

[10] J. I. S. Hummel, "Winch Sizing for Ground-Generator Airborne Wind Energy Systems," https://github.com/jesseishi/AWE_winch_sizing, Mar. 2024.

[11] A. U. Zgraggen, L. Fagiano, and M. Morari, "Automatic Retraction and Full-Cycle Operation for a Class of Airborne Wind Energy Generators," *IEEE Transactions on Control Systems Technology*, vol. 24, no. 2, pp. 594–608, Mar. 2016.

[12] R. H. Luchsinger, "Pumping Cycle Kite Power," in *Airborne Wind Energy*, ser. Green Energy and Technology, U. Ahrens, M. Diehl, and R. Schmehl, Eds. Berlin, Heidelberg: Springer Berlin Heidelberg, 2013, pp. 47–64.

[13] A. Berra and L. Fagiano, "An optimal reeling control strategy for pumping airborne wind energy systems without wind speed feedback," in *2021 European Control Conference (ECC)*. Delft, Netherlands: IEEE, June 2021, pp. 1199–1204.

[14] D. Eijkelhof, S. Rapp, U. Fasel, M. Gaunaa, and R. Schmehl, "Reference Design and Simulation Framework of a Multi-Megawatt Airborne Wind Energy System," *Journal of Physics: Conference Series*, vol. 1618, no. 3, Sept. 2020.

[15] P. Williams, "Cable Modeling Approximations for Rapid Simulation," *Journal of Guidance, Control, and Dynamics*, vol. 40, no. 7, pp. 1779–1788, July 2017.

[16] S. Rapp, R. Schmehl, E. Oland, and T. Haas, "Cascaded Pumping Cycle Control for Rigid Wing Airborne Wind Energy Systems," *Journal of Guidance, Control, and Dynamics*, vol. 42, no. 11, pp. 2456–2473, Nov. 2019.

[17] J. I. S. Hummel, T. S. C. Pollack, D. Eijkelhof, E.-J. Van Kampen, and R. Schmehl, "Power smoothing by kite tether force control for megawatt-scale airborne wind energy systems," *Journal of Physics: Conference Series (accepted)*, 2024.

[18] L. V. Hagen, K. Petrick, S. Wilhelm, and R. Schmehl, "Life-Cycle Assessment of a Multi-Megawatt Airborne Wind Energy System," *Energies*, vol. 16, p. 1750, Feb. 2023.

[19] J. Jonkman, S. Butterfield, W. Musial, and G. Scott, "Definition of a 5-MW Reference Wind Turbine for Offshore System Development," National Renewable Energy Laboratory (NREL), Tech. Rep. NREL/TP-500-38060, Feb. 2009.